Journal of Physical Chemistry and Functional Materials

Home Page of Journal: https://dergipark.org.tr/jphcfum

Synthesis and Optical Properties of 2-(4-trifluoromethylphenyl)-3-(4-methoxyphenyl) Acrylonitrile (4MPAN-TFMP) Compound

Leyla Babali Özen[a]*, Furkan Özen[b] , Bayram Gündüz[c] and Günseli Turgut Cin[a]

[a] *Akdeniz University, Department of Chemistry, Antalya, Turkey*
[b] *Akdeniz University,Department of Mathematics and Science, Faculty of Education, Antalya, Turkey*
[c]*Department of Engineering Basic Sciences, Faculty of Engineering and Natural Sciences, Malatya Turgut Özal University, 44900 Malatya, Türkiye*
** Corresponding author: E-mail: leyla.babaliozen1@gmail.com*

ABSTRACT

The 2-(4-Trifluoromethylphenyl)-3-(4-methoxyphenyl) acrylonitrile (4MPAN-TFMP) compound was successfully synthesized and characterized using standard spectroscopic methods. Thin films of 4MPAN-TFMP were prepared by conventional spin-coating, with varying film thicknesses to investigate the thickness-dependent optical and photonic properties. UV-Vis spectra of the compounds in DMSO were recorded, and key parameters such as absorption (Abs), transmittance (T), absorption band edge ($E_{Abs\text{-}be}$), optical band gap (E_g), and refractive index (n) were determined. The findings highlight the material's potential for optoelectronic applications, as optimized film thicknesses can enhance material efficiency for various uses. This advancement offers promising implications for developing high-performance photonic devices and improving optoelectronic circuit components.

ARTICLE INFO

Keywords:
Acrylonitriles
Organic Semiconductors
Photonic Properties
Optoelectronic applications
Film thickness

Received: 2024-11-12
Accepted: 2024-12-08
ISSN: 2651-3080
DOI: 10.54565/jphcfum.1583947

1. INTRODUCTION

Interest in conjugated materials has grown remarkably over the past two decades, driving extensive research and development across various optoelectronic devices. Conjugated molecules with electron donor-acceptor structures have attracted particular attention due to their unique photochemical properties and efficient intramolecular charge transfer, which make them promising candidates for optoelectronic applications. [1, 2]. The energy levels of the organic molecules are defined by the highest occupied molecular orbital (HOMO, energy EH) and the lowest unoccupied molecular orbital (LUMO, energy EL). When an exciton reaches the heterojunction and its energy step is sufficient to exceed the exciton binding energy, it can be split into an electron on the acceptor side and a hole on the donor side [3]. Research continues to optimize the energy alignment between the LUMO (or HOMO) levels of the donor and acceptor relative to the exciton energy to improve optoelectronic material efficiency [4,5].

Recent studies indicate that exciton dissociation is influenced by several factors, including energy

configuration, temperature, fabrication methods, layer thickness, and molecular structure and arrangement [6-8]. Acrylonitrile compounds, as a subset of conjugated molecules with electron donor-acceptor structures, also exhibit significant photophysical properties [9].

Organic semiconductors are widely employed in optoelectronic devices due to their versatile chemical structures, which allow for structural modifications The design and synthesis of these organic semiconductor materials to enable solution processing through methods like spin coating, inkjet printing, and screen printing—combined with their compatibility with flexible substrates and potential for enhanced optical properties—are key factors driving interest in this field [11, 12]. Consequently, applications such as smart organic optoelectronic materials [13], organic thin-film transistors (TFTs) [14], organic solar cells and photovoltaic devices [15-17], semiconductor devices [18], and organic light-emitting diodes (OLEDs) [19, 20] have increased the focus on designing and synthesizing such compounds.

Electron-donating and electron-accepting π-conjugated compounds such as carbazole [21], pyrene [22], triazole [23] and chalcone [24] have been reported to form donor-π-acceptor (D-π-A) systems. Extensive research on these systems has provided valuable information on their photophysical properties. Investigation of the photonic properties of these systems is crucial for understanding the surface/interface interaction mechanisms in optoelectronic devices. However, studies of the interaction mechanisms of acrylonitrile compounds in this context are limited.

In this study, 2-(4-trifluoromethylphenyl)-3-(4-methoxyphenyl) acrylonitrile (4MPAN-TFMP) was synthesized via the Knoevenagel condensation method. This reaction, performed under basic conditions (NaOH, KOH, NaOEt, and K_2CO_3) in polar solvents (MeOH or EtOH), is a conventional approach for synthesizing aryl acrylonitrile derivatives [25]. The significant optical properties of α, β-unsaturated conjugated organic compounds highlight the importance of understanding structure-property relationships in these molecules. Thin films of the synthesized 4MPAN-TFMP were prepared with varying thicknesses using spin-coating, and potential applications of the molecule in chemical sensors and optoelectronic materials were evaluated. This work thus contributes to the development of materials with promising future applications in these fields.

2. MATERIAL AND METHOD

2.1. Synthesis of 2-(4-Trifloromet ilfenil)-3-(4-metoksifenil)akrilonitril (4MPAN-TFMP) Compound

4-Methoxybenzaldehyde (1) (3.67 mmol) and 3-trifluoromethylphenyl acetonitrile (2) (3.67 mmol) were added to a 20 mL ethanol solution, and the mixture was processed according to the method described in the literature [26,27]. The synthesis of 4MPAN-TFMP is illustrated in Scheme 1. Yield: 0.47 g. 94 *%. Anal. Calc.* for $C_{17}H_{12}F_3NO$ (MW= 303.28): C, 67.33; H, 3.99; N, 4.62. Found: C, 67.28; H, 3.95; N, 4.62.

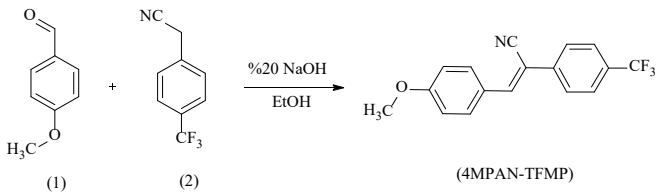

Scheme 1. General synthesis scheme of compound

The synthesized compound was characterized by elemental analysis, FT-IR, ^{1}H-NMR and ^{13}C-APT-NMR spectroscopic techniques.

FT-IR (KBr, *cm^{-1}*): 3059 and 3023$\nu_{C\text{-}H(Ar.)}$, 2214$\nu_{C\equiv N}$, 1563 and 1595$\nu_{C=C}$ *and* 920$\nu_{C\text{-}F}$.

^{1}H-NMR (400 *MHz*, $CDCl_3$-d_1) *δ/ppm*: 3.92 (3H, s, H^1), 7.03 (2H, d, J=8.8, H^3), 7.57 (1H, s, H^6), 7.72 (2H, d, j=8.4, H^{10}), 7.78 (2H, d, j=8.0, H^{11}) and 7.96 (2H, d, j=8.8, H^4).

^{13}C-APT-NMR (400 *MHz* $CDCl_3$-d_1) *δ/ppm*: 55.51 C^1, 107.12 C^7, 114.56 C^3, 118.07 C^8, 126.04 C^{11}, 121.86 C^5, 130.57 C^9, 130.73 C^{10}, 131.60 C^4, 138.37 C^{12}, 143.75 C^6, 161.99 C^2.

2.2. Preparation and Optical Characterization of 4MPAN-TFMP Films

The 4MPAN-TFMP semiconductor solution was prepared by dissolving the compound in DMSO, with thorough mixing via a vortex mixer to ensure solution homogeneity. Glass substrates were cut with a diamond cutter and

cleaned by sequential washing in deionized water (DIW) and hydrochloric acid (HCl) to remove glass particles and contaminants. Following this, the substrates were rinsed with DIW to eliminate HCl residues and with ethanol to remove organic impurities, then dried with pressurized nitrogen.

The 4MPAN-TFMP films were deposited onto the cleaned, dried glass substrates using the spin-coating technique. After coating, the films were allowed to sit at room temperature for 8 minutes to ensure solvent evaporation. Three different 4MPAN-TFMP film thicknesses were prepared and measured using a thickness gauge (ASIMETO model) as 7.69, 13.77 and 32.45 µm, respectively.

The optical properties of 4MPAN-TFMP films were investigated by UV measurements at room temperature in the wavelength range 1100-190 nm. This analysis of films with varying thicknesses allowed for the determination of key optical parameters, including optical band gaps, absorption, conductivity, and refractive index. Such detailed optical characterization offers valuable insights into the potential applicability of 4MPAN-TFMP films in optoelectronic devices.

3. RESULTS AND DISCUSSIONS

3.1. Experimental Photonic and Refractive Index Characteristics of 4MPAN-TFMP Films

Optical absorption measurements are widely used to study photonic and optoelectronic properties. These measurements have been used to determine the interaction between light and 4MPAN-TFMP films. Techniques such as UV-visible (UV-Vis) or electronic absorption spectroscopy are among the most effective methods for investigating these properties [29]. **Figure 1** presents the absorption spectra of the 4MPAN-TFMP material in DMSO at film thicknesses of 7.69, 13.77 and 32.45 µm, showing a maximum absorption peak around 347 nm. As expected, absorption increases with film thickness, while above 400 nm, absorption remains minimal and constant.

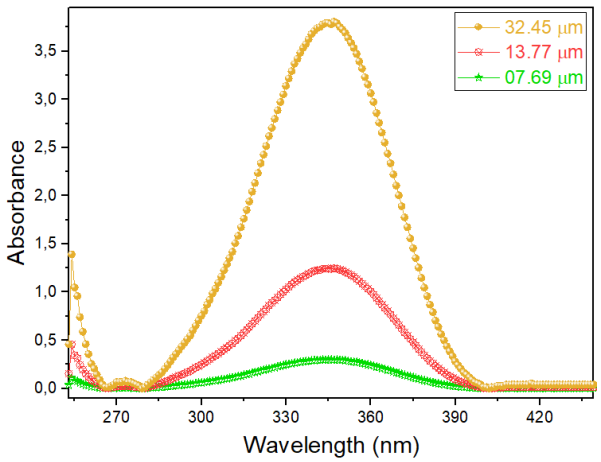

Figure 1 The absorbance spectra of the 4MPAN-TFMP material in DMSO at different film thicknesses.

The transmittance spectra of 4MPAN-TFMP films with the same thicknesses are illustrated in **Figure 2**. The transmittance values exhibit a sharp increase following a dip around 345 nm, reaching a peak near 400 nm. Transmittance decreases as film thickness increases, as anticipated.

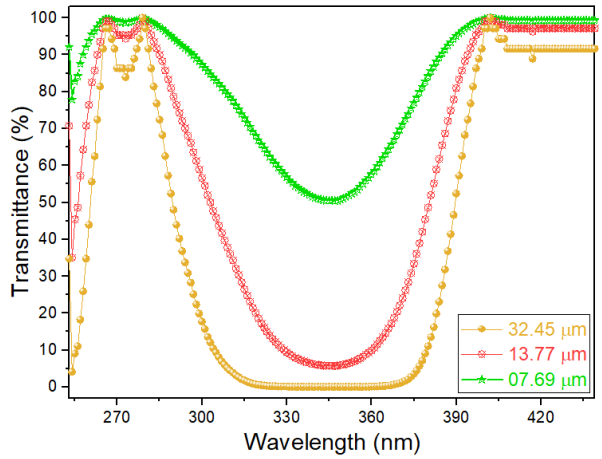

Figure 2 The transmittance spectra of the 4MPAN-TFMP material in DMSO at different film thicknesses.

The absorption band edge values, calculated from the first derivative of the transmittance curve (**Figure 3**), were 3.131, 3.108, and 3.092 eV for film thicknesses of 7.69, 13.77, and 32.45 µm, respectively. These values indicate a decreasing absorption band edge with increasing film thickness, with the lowest absorption band edge observed at 32.45 µm.

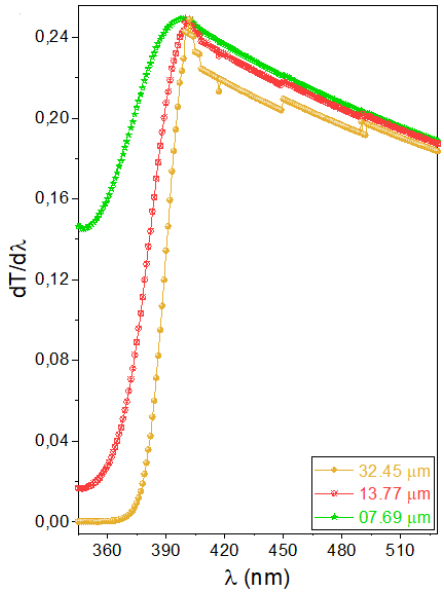

Figure 3 dT/dλ vs. λ curves of the 4MPAN-TFMP films for 7.69, 13.77, and 32.45 µm film thicknesses.

The optical band gap (Eg) is a key parameter for photonic and optoelectronic applications. The optical band gap values of the 4MPAN-TFMP molecule for film thicknesses of 7.69, 13.77 and 32.45 µm were calculated using the $(\alpha h\nu)^2$ plot versus photon energy as shown in **Figure 4**. Results indicate that the E_g value decreases with increasing film thickness, with the lowest E_g (3.109 eV) at 32.45 µm and the highest E_g (3.223 eV) at 7.69 µm. This trend suggests that the optical band gap of 4MPAN-TFMP films decreases as thickness increases, highlighting their potential for optoelectronic applications.

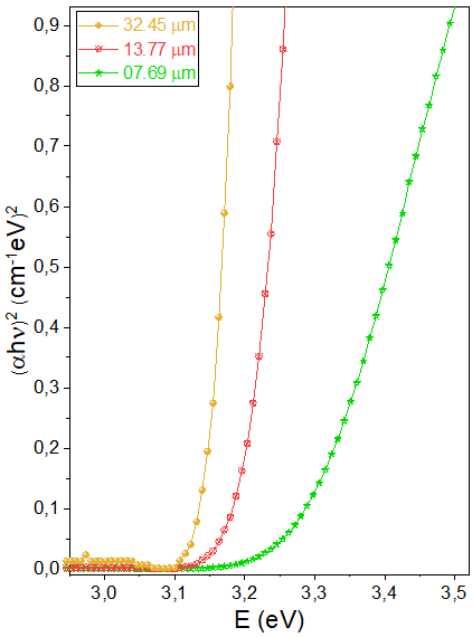

Figure 4 The $(\alpha h\nu)^2$ plot versus photon energy (E) of the 4MPAN-TFMP films for 7.69, 13.77 and 32.45 film thicknesses.

The investigation of the αc parameter, widely used in sensor, is considered a significant finding that highlights the practical potential of this study. The sensing properties of 4MPAN-TFMP materials with different film thicknesses were examined using the contrast (αc) parameter, which is crucial for sensor technologies. This parameter indicates the sensing capabilities of a material and can be calculated using the following formula:

$$\alpha_c = 1 - \left(\frac{n_1}{n_2}\right)^2 \quad (1)$$

The details and results of this equation aid in understanding the photophysical properties of the material. Here, n_1 and n_2 are the refractive indices of the medium and the solution, respectively. The αc values of the 4MPAN-TFMP molecule for different film thicknesses were calculated, and the corresponding αc curves were plotted against E, in the graph as shows in **Figure 5.** It is observed that the 4MPAN-TFMP molecule shows a sharper and more stable sensitivity to increasing photon energy with increasing film thickness. This finding shows that the material has photosensitive properties and is a promising candidate for optoelectronic devices.

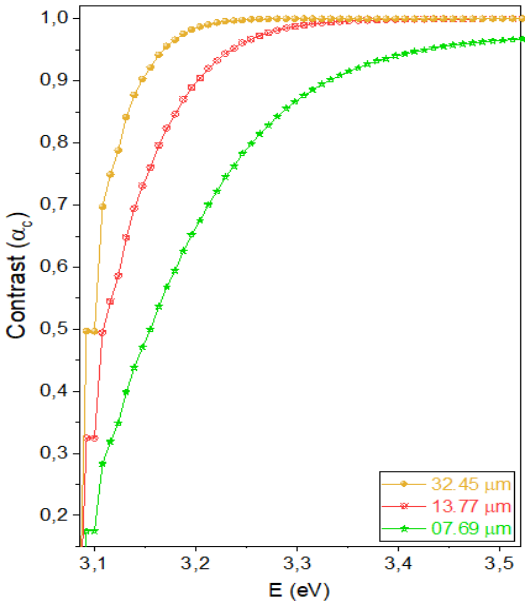

Figure 5. The contrast (αc) curves of the 4MPAN-TFMP molecule against photon energy (E) for film thicknesses of 7.69, 13.77, and 32.45 µm.

Reflectance spectra are an important method for understanding the optical properties of a material because they provide information about the interaction of the material with light. In order to obtain the optical refractive index (n) values, various equations such as Reddy, Ravindra, Kumar-Singh, Herve-Vandamme and Moss [29] were used for 4MPAN-TFMP films at film thicknesses of 7.69, 13.77, and 32.45 µm. These equations were directly applied along with the optical band gap (E_g) values. These calculated values are presented in Table 1. It is observed that the refractive indices increase with increasing film thickness.

Tablo 1 The refractive index values of the 4MPAN-TFMP molecule obtained from various relations for film thicknesses of 7.69, 13.77, and 32.45 µm.

Film Thickness (µm)	Refractive Index Values				
	Moss	Ravindra	Herve-Vandamme	Reddy	Kumar-Singh
32.45	2.351	2.156	2.296	2.737	2.336
13.77	2.344	2.133	2.286	2.728	2.327
7.69	2.330	2.086	2.265	2.709	2.309

Average n values for these relations were also calculated, and Figure 6 displays the refractive index curves for different film thicknesses, further illustrating this trend.

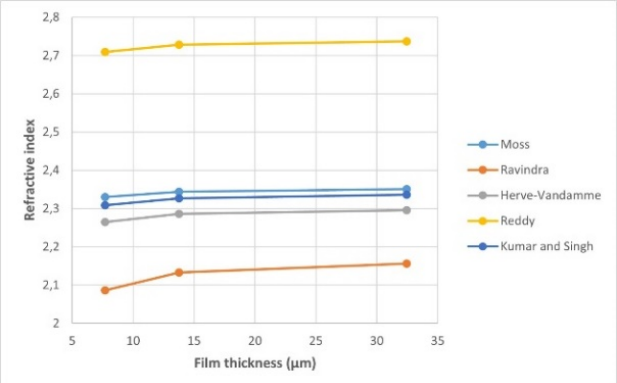

Figure 6 Refractive index *n* curves for 4MPAN-TFMP organic material at different film thicknesses for different relations.

The results obtained show that the refinement of the optical parameters studied at different film thicknesses provides a flexible and comprehensive approach for modelling layered systems with different degrees of coherence. This method proves to be an effective tool for investigating the effects of film thickness on the electrical and optical properties of thin film materials. The study has shown that the increase in film thickness has a consistent relationship between the energy band gap (Eg) and the band edge values, in accordance with the desired properties in optical material designs such as OLEDs, LEDs, photodetectors and solar cells [30-32]. These materials can be optimized for specific applications through the tailoring of energy levels in order to increase their photovoltaic performance [33]. Furthermore, the observed increase in contrast and refractive index values with increasing film thickness is considered a critical parameter for the design and fabrication of photosensitive optoelectronic devices, especially laser diodes, sensors, and fiber optic devices [34,36]

4. DISCUSSION

The electrical conductivity or carrier density of thin films under UV light can be enhanced depending on the structure of the material and the charge movement under the electric field. Thus, optimizing parameters such as coating technique, surface roughness, and film thickness is essential, and their effects warrant thorough investigation. In this study, thin films of 4MPAN-TFMP with varying thicknesses were prepared via the spin-coating method, and the photonic properties of this organic semiconductor material were examined in relation to absorption parameters under UV-Vis light. The films exhibited an indirect allowed optical band gap from 3.223 eV to 3.109 eV, which decreases from 3.223 eV to 3.109 eV as the film thickness increases from 0.769 µm to 32.45 µm. Additionally, the contrast and refractive index values increase with increasing film thickness, suggesting promising results in the production of photosensitive optoelectronic devices.

Acknowledgement: We would like to thank the Scientific and Technological Research Council of Turkey (TÜBİTAK, KBAG-119Z608) and Akdeniz University Scientific Research Projects Unit (AU-BAP, FBA-2020-5403 and FDK-2022-6056) for their financial support.

Competing interests

The authors declare that they have no competing interests.

REFERENCES

[1] Roncali, J. (2011). Single material solar cells: the next frontier for organic photovoltaics. Advanced Energy Materials, 1(2), 147-160.

[2] Wang, Y., Shang, H., Li, B., & Jiang, S. (2022). Reversible luminescence "off–on" regulation based on tunable photodimerization via crystal-to-cocrystal transformation. Journal of Materials Chemistry C, 10(2), 734-741.

[3] Dolomanov, O. V., Bourhis, L. J., Gildea, R. J., Howard, J. A., & Puschmann, H. (2009). OLEX2: a complete structure solution, refinement and analysis program. Journal of applied crystallography, 42(2), 339-341.

[4] Strieth-Kalthoff, F., James, M. J., Teders, M., Pitzer, L., & Glorius, F. (2018). Energy transfer catalysis mediated by visible light: principles, applications, directions. Chemical Society Reviews, 47(19), 7190-7202.

[5] Zhou, Q. Q., Zou, Y. Q., Lu, L. Q., & Xiao, W. J. (2019). Visible-light-induced organic photochemical reactions through energy-transfer pathways. Angewandte Chemie International Edition, 58(6), 1586-1604.

[6] Gündüz, B. (2013). Effects of molarity and solvents on the optical properties of the solutions of tris [4-(5-dicyanomethylidenemethyl-2-thienyl) phenyl] amine (TDCV-TPA) and structural properties of its film. Optical Materials, 36(2), 425-436.

[7] Lloyd, M. T., Anthony, J. E., & Malliaras, G. G. (2007). Photovoltaics from soluble small molecules. Materials Today, 10(11), 34-41.

[8] Anandhan, K., Cerón, M., Perumal, V., Ceballos, P., Gordillo-Guerra, P., Pérez-Gutiérrez, E., ... & Percino, M. J. (2019). Solvatochromism and pH effect on the emission of a triphenylimidazole-phenylacrylonitrile derivative: experimental and DFT studies. RSC advances, 9(21), 12085-12096.

[9] Castillo, A., Ceballos, P., Santos, P., Cerón, M., Venkatesan, P., Pérez-Gutiérrez, E., ... & Percino, M. J. (2021). Solution and solid-state photophysical properties of positional Isomeric acrylonitrile derivatives with Core pyridine and phenyl moieties: experimental and DFT studies. Molecules, 26(6), 1500.

[10] Jayabharathi, J., Thanikachalam, V., & Perumal, M. V. (2012). Physicochemical and solvatochromic analysis of an imidazole derivative as NLO material. Spectrochimica Acta Part A: Molecular and Biomolecular Spectroscopy, 85(1), 31-37.

[11] Büchele, P., Richter, M., Tedde, S. F., Matt, G. J., Ankah, G. N., Fischer, R., ... & Schmidt, O. (2015). X-ray imaging with scintillator-sensitized hybrid organic photodetectors. Nature Photonics, 9(12), 843-848.

[12] Hssain, A. H., Gündüz, B., Majid, A., & Bulut, N. (2021). NTCDA compounds of optoelectronic interest: Theoretical insights and experimental investigation. Chemical Physics Letters, 780, 138918.

[13] Zhu, L., & Zhao, Y. (2013). Cyanostilbene-based intelligent organic optoelectronic materials. Journal of Materials Chemistry C, 1(6), 1059-1065.

[14] Kim, M. J., An, T. K., Kim, S. O., Cha, H., Kim, H. N., Xiofeng, T., ... & Kim, Y. H. (2015). Molecular design and ordering effects of alkoxy aromatic donor in a DPP copolymer on OTFTs and OPVs. Materials Chemistry and Physics, 153, 63-71.

[15] Fang, J. K., Sun, T., Tian, Y., Zhang, Y., Jin, C., Xu, Z., ... & Wang, H. (2017). Novel diyne-bridged dyes for efficient dye-sensitized solar cells. Materials Chemistry and Physics, 195, 1-9.

[16] Shaikh, S. A., Mendhe, A. C., Nadimetla, D. N., Biradar, M. R., Vijayanand, P., Puyad, A. L., ... & Bhosale, S. V. (2024). Benzothiazole functionalized diketopyrrolopyrrole photosensitizer for CdS nanowire based DSSC applications. Journal of Photochemistry and Photobiology A: Chemistry, 447, 115220.

[17] Sharma, G. D., Patel, K. R., Roy, M. S., & Misra, R. (2014). Characterization of two new (A–π) 2–D–A type dyes with different central D unit and their application for dye sensitized solar cells. Organic Electronics, 15(8), 1780-1790.

[18] Jeong, H. G., Khim, D., Jung, E., Yun, J. M., Kim, J., Ku, J., ... & Kim, D. Y. (2013). Synthesis and characterization of a novel ambipolar polymer semiconductor based on a fumaronitrile core as an electron-withdrawing group. Journal of Polymer Science Part A: Polymer Chemistry, 51(5), 1029-1039.

[19] Gündüz, B. (2016). Investigation of the spectral, optical and surface morphology properties of the N, N′-Dipentyl-3, 4, 9, 10-perylenedicarboximide small molecule for optoelectronic applications. Polymers For Advanced Technologies, 27(2), 144-155.

[20] Imer, A. G., Kaya, E., Dere, A., Al-Sehemi, A. G., Al-Ghamdi, A. A., Karabulut, A., & Yakuphanoglu, F. (2020). Illumination impact on the electrical characteristics of Au/Sunset Yellow/n-Si/Au hybrid Schottky diode. Journal of Materials Science: Materials in Electronics, 31, 14665-14673.

[21] Jhulki, S., & Moorthy, J. N. (2018). Small molecular hole-transporting materials (HTMs) in organic light-emitting diodes (OLEDs): Structural diversity and classification. Journal of Materials Chemistry C, 6(31), 8280-8325.

[22] Wrona-Piotrowicz, A., Ciechańska, M., Zakrzewski, J., & Makal, A. (2016). Pyrene fluorophores bearing two carbonyl groups in 1, 2-positions: Synthesis and photophysical properties of pyrene-1, 2-dicarboximides and a pyrene-1, 2-dicarboxamide. *Journal of Photochemistry and Photobiology A: Chemistry*, *330*, 15-21.

[23] Santana-Martínez, I., Ramírez-Palma, M. T., Sánchez-Escalera, J., Martínez-Otero, D., García-Eleno, M. A., Dorazco-González, A., & Cuevas-Yañez, E. (2020). Synthesis, structural analysis, and photophysical properties of bi-1, 2, 3-triazoles. *Structural Chemistry*, *31*, 191-201.

[24] Coskun, D., Gunduz, B., & Coskun, M. F. (2019). Synthesis, characterization and significant optoelectronic parameters of 1-(7-methoxy-1-benzofuran-2-yl) substituted chalcone derivatives. *Journal of molecular structure*, *1178*, 261-267.

[25] Guillot, R., Loupy, A., Meddour, A., Pellet, M., & Petit, A. (2005). Solvent-free condensation of arylacetonitrile with aldehydes. **Tetrahedron, 61(4**2), 10129-10137.

[26] Buu-Hoi, N. P., Saint-Ruf, G., & Lobert, B. (1969). Oxygen heterocycles. Part XIV. Hydroxylated 3-aryl-and 3-pyridyl-coumarins. Journal of the Chemical Society C: Organic, (16), 2069-2070.

[27] Yakalı, G., Çoban, M. B., Özen, F., Özen, L. B., Gündüz, B., & Cin, G. T. (2021). The importance of polymorphism dependent aggregation induced enhanced emission of the acrylonitrile derivative: Helical J type and antiparallel h type stacking modes. ChemistrySelect, 6(41), 11392-11406.

[28] Zhang, J. Z. (2009). Optical properties and spectroscopy of nanomaterials. World Scientific.

[29] Tripathy, S. K. (2015). Refractive indices of semiconductors from energy gaps. Optical materials, 46, 240-246.

[30] El-Menyawy, E. M., Elagamey, A. A., Elgogary, S. R., & El-Enein, R. A. (2013). Optical, electrical and photovoltaic properties of thermally evaporated 3-amino-2-[(2-nitrophenyl) diazinyl]-3-(piperidin-1-yl) acrylonitrile thin films. Materials science in semiconductor processing, 16(6), 1828-1836.

[31] Zeyada, H. M., El-Nahass, M. M., & El-Shabaan, M. M. (2016). Photovoltaic properties of the 4H-pyrano [3, 2-c] quinoline derivatives and their applications in organic–inorganic photodiode fabrication. *Synthetic Metals*, *220*, 102-113.

[32] Cheng, P., & Zhan, X. (2016). Stability of organic solar cells: challenges and strategies. Chemical Society Reviews, 45(9), 2544-2582.

[33] Riede, M., Mueller, T., Tress, W., Schueppel, R., & Leo, K. (2008). Small-molecule solar cells—status and perspectives. Nanotechnology, 19(42), 424001.

[34] Khapre, A., Kumar, A. V., & Chandrasekar, R. Powering Organic Flexible Optical Waveguides and Circuits via Focused Micro-LEDs for Visible Light Communication. *Laser & Photonics Reviews*, 2400278.

[35] Görrn, P., Lehnhardt, M., Kowalsky, W., Riedl, T., & Wagner, S. (2011). Elastically tunable self-organized organic lasers. *Advanced Materials*, *23*(7), 869.**[36]** Seemann, A., Sauermann, T., Lungenschmied, C., Armbruster, O., Bauer, S., Egelhaaf, H. J., & Hauch, J. (2011). Reversible and irreversible degradation of organic solar cell performance by oxygen. *Solar Energy*, *85*(6), 1238-1249.